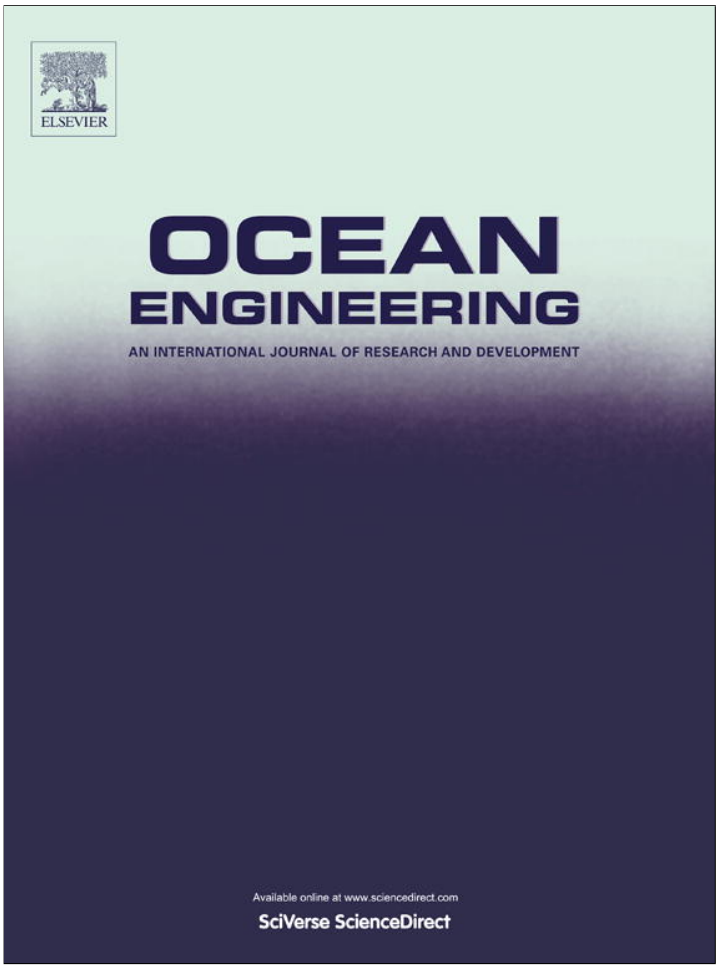

(This is a sample cover image for this issue. The actual cover is not yet available at this time.)

Ocean Engineering 53 (2012) 16–24

Contents lists available at SciVerse ScienceDirect

Ocean Engineering

journal homepage: www.elsevier.com/locate/oceaneng

Dynamics of the container crane on a mobile harbor

Keum-Shik Hong [a,b,*], Quang Hieu Ngo [b]

[a] Department of Cogno-Mechatronics Engineering, Pusan National University, 30 Jangjeon-dong, Geumjeong-gu, Busan 609-735, Republic of Korea
[b] School of Mechanical Engineering, Pusan National University, 30 Jangjeon-dong, Geumjeong-gu, Busan 609-735, Republic of Korea

ARTICLE INFO

Article history:
Received 30 April 2011
Accepted 9 June 2012
Editor-in-Chief: A.I. Incecik

Keywords:
Offshore crane
Dynamic model
Mobile harbor
Wave-induced motion
Sea State 3

ABSTRACT

In this paper, a dynamic model of a ship-mounted container crane (called the "mobile harbor") subject to the motions of ship itself imparted by random sea waves is investigated. The condition of the sea is assumed to be State 3. The ship's heaving, pitching and rolling motions are considered as the main motions in exciting the mounted crane. Equations of motion are derived using the Lagrange method. Simulation results reveal that the lateral sway angle of the load becomes the biggest in the beam sea, whereas the pitching motion of the ship in the heading sea is the biggest. As a conclusion, the operation of mobile harbors in the heading sea is recommended. The developed mathematical model has been validated by experiments.

1. Introduction

Container cranes are widely used to transfer containers and other objects from and to various locations in ports and at container terminals. In recent years, with the rapid growth of the world logistics industry and the attendant rises in competition and costs, ship companies have resorted to making container ships larger. Presently, container ships over the 12,000 TEU (20-foot equivalent unit) class are plying the main trunk routes, and still-larger, 15,000 TEU class ships are on order. It is predicted that by the 2020s, super large, 18,000 TEU container ships will be in operation. So as to keep up with ever-increasing ship sizes, container cranes have to become larger, faster, and higher, necessitating, in turn, efficient controllers that can both guarantee fast turn-over times and meet stringent safety requirements. Despite these improvements, one problem has remained for small container terminals and ports: they cannot accommodate, owing to their relatively shallow water depths, the larger container ships. To solve this problem, a special crane-equipped ship ("mobile harbor") capable of operating on the open sea has been proposed (however, a complete efficiency study has not been made yet). Fig. 1 shows a mobile harbor that loads and unloads containers from a mega container ship in an open sea.

In the process of loading/unloading containers, the longitudinal and lateral motions of the trolley (especially when starting or stopping, along with wave-induced ship movement) impart a pendulum motion to the suspended container. This not only leads to a potentially serious damage that can result, but also prolongs the time required to precise positioning of the load. A satisfactory control method for suppression of the motion of the container being transferred, therefore, is a necessity for crane engineers. Besides that, crane system dynamics must be clarified before designing a control system. Therefore, the dynamics analysis of the plant is the first step to develop any crane's control system.

The container, hooked to a spreader, is suspended in air by four ropes. When the container is accelerated by the trolley or disturbed by winds, it may exhibit a rotational motion (trim, list, skew) as well as a sway in the vertical plane. Depend on different points of view or different purposes, the container crane can be modeled by many ways. When the sway motion of the spreader was modeled as a pendulum motion, lumped parameter system approaches were developed (Singhose et al., 2000; Hong et al., 2000; Kim et al., 2004; Lee, 2004; Liu et al., 2005; Park et al., 2007; Singhose and Kim, 2008; Ngo and Hong, 2009, 2012a). Also, when the flexibility of the ropes was focused, distributed parameter system approaches were investigated (d'Andrea-Novel and Coron, 2000; Rahn et al., 2000; Fang et al., 2003; Choi et al., 2004; Kim and Hong, 2009; Ngo et al., 2009).

A floating crane (a crane mounted on a ship) has been also investigated. Ellermann and Kreuzer (2003) investigated the dynamics of a floating crane that exhibits various nonlinear phenomena. Ngo and Hong (2012b) developed the first mathematical model of the container crane mounted on a ship with predefined motions. Besides the above, the interactions between ocean structures and waves were intense research issues for other

* Corresponding author at: Department of Cogno-Mechatronics Engineering, Pusan National University, 30 Jangjeon-dong, Geumjeong-gu, Busan 609-735, Republic of Korea. Tel.: +82 51 510 2454; fax: +82 51 514 0685.
E-mail addresses: kshong@pusan.ac.kr (K.-S. Hong), nqhieu@pusan.ac.kr (Q.H. Ngo).

0029-8018/$ - see front matter © 2012 Elsevier Ltd. All rights reserved.
http://dx.doi.org/10.1016/j.oceaneng.2012.06.013

researchers (Zhu et al., 2001; Love et al., 2003; Kyoung et al., 2005; Park et al., 2006; Do and Pan, 2008; Clauss et al., 2009; Cha et al., 2010; Lee et al., 2010; VanZwieten et al., 2010a,b).

This paper focuses on the dynamics analysis of the crane mounted on a ship, which is subject to random waves in Sea State 3. The contributions of this paper are the following: A dynamic model of the ship-mounted container crane subject to the ship motions (imparted by random waves) is derived for the first time. Equations of motion, including the ship motion, are acquired using the Lagrange method and are validated by experiment. The effects of the wave-induced motions on the free-swinging load are analyzed, in which the sea wave direction is considered as a main factor in determining the orientation of the mother ship for mobile harbor operations in the open sea. It is found that the beam sea generates the coupled motions of the longitudinal and lateral sway motions of the load, and the heading sea results in the minimal sway of the load in contrast to the big pitching motion of the ship itself.

The paper is organized as follows. In Section 2, the dynamics of a ship-mounted container crane is investigated. Environmental disturbances from sea waves are defined, the kinematical transformation matrices are presented, and the Lagrange equation is used to derive the equations of motion, including those of the container crane (and load) mounted on the ship. In Section 3, the numerical simulation results for the ship motion and the sway angle of the container are discussed. The simulation compares the random waves in three directions (heading sea, quartering sea, and beam sea) in order to better analyze the effects of wave directions for safe loading and unloading. Finally, in Section 4, conclusions are drawn and future work is proposed.

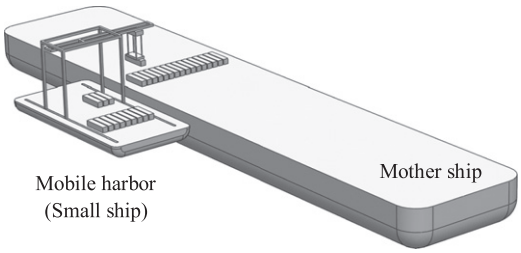

Fig. 1. Loading/unloading of containers at a mobile harbor in an open sea.

2. Modeling of a ship-mounted container crane

2.1. Coordinate systems

Fig. 2 depicts the three coordinate systems introduced to describe the motion of a ship-mounted container crane. Let $O_n - x_n y_n z_n$ denote the inertial coordinate frame, which becomes the reference frame that is apart from the mother ship by a fixed distance. Let $O_s - x_s y_s z_s$ be the ship coordinate frame affixed to the hull of the mobile harbor in which the origin O_s is located at the center of gravity of the mobile harbor. The axes of the ship coordinate frame are chosen to coincide with the principal axes (surge, sway, and heave) of the mobile harbor. Also, O_n, which is located underneath the O_s, is assumed to be located at the mean water free-surface. Finally, let $O_t - x_t y_t z_t$ be the trolley coordinate frame affixed to the trolley. The positive x_t-axis indicates the forward movement of the entire crane toward the surge direction of the ship, the positive y_t-axis expresses the trolley's movement toward the mother ship along the boom, and the positive z_t-axis denotes the upward direction to the sky. Besides these three frames, the hydrodynamic frame is sometimes introduced for computing the interaction forces (for instance, Froude–Krilov force) caused by the waves, but the coincidence of the hydrodynamic frame and the inertial frame is assumed in our case, since all the ships are not in motion (i.e., not propelled) during loading/unloading.

2.2. Wave disturbances

The suppression of payload oscillations is especially important in the case of a mobile harbor. The wave-induced ship motions can contain enough energy near the natural frequency of the free-swinging load, which can impart large motions to the load directly or indirectly by creating motion instability. Ocean waves are random in both time and space. A conceptual model describing the elevation of an irregular sea considers the sum of a large number of essentially independent regular (sinusoidal) contributions with random phases. Accordingly, the sea elevation at location

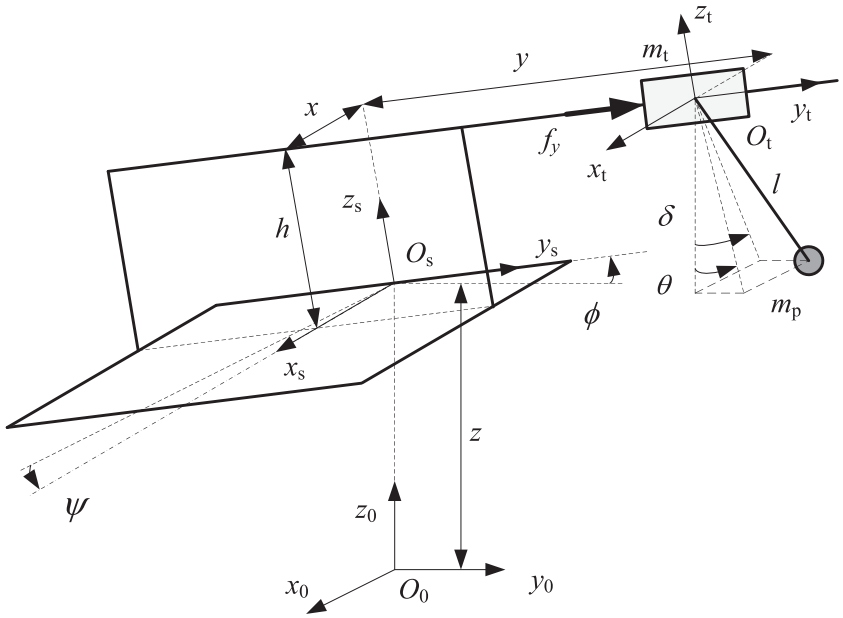

Fig. 2. Introduced coordinate frames: inertial, ship, and trolley.

x, y with respect to the inertial frame is given by

$$\zeta(x,y,t) = \sum_{i=0}^{N} \zeta_i(x,y,t)$$

$$= \sum_{i=0}^{N} \overline{\zeta}_i \sin(\omega_i t + \theta_i - k_i x \cos\chi - k_i y \sin\chi), \quad (1)$$

where $\zeta_i(x,y,t)$ is the contribution of the regular or harmonic travelling waves component i propagating at angle χ with respect to the inertial frame and with a random phase θ_i with uniform distribution on the interval $[-\pi, \pi]$. k_i, ω_i, and $\overline{\zeta}_i$ are the wave number, wave frequency, and wave amplitude, respectively, of component i and are calculated by the following equations:

$$k_i = \frac{2\pi}{\lambda_i}, \quad \omega_i = \sqrt{gk_i} = \frac{g}{c_i}, \quad c_i = \sqrt{\frac{g\lambda_i}{2\pi}}, \quad (2)$$

where λ_i is the wavelength and c_i is the wave celerity of component i.

Since the standard waves are characterized as combinations of wave amplitudes and frequencies, it is practical to model the wave motions as an energy spectrum. There are several standards for defining sea conditions. Here, we use the modified Pierson–Moskowitz family, recommended at the 15th International Towing Tank Conference (ITTC) in 1978. Thus, the wave spectral density is defined as

$$S_{\zeta\zeta}(\omega) = \frac{A}{\omega^5} \exp\left(\frac{-B}{\omega^4}\right), \quad (3)$$

where $A = 173H_{1/3}^2/T^4$, $B = 691/T^4$, $H_{1/3}$ is the significant wave height, and T is the average period (Perez, 2005).

2.3. Ship motions

The response of a ship to waves is very complex. The ship motion of six degrees of freedom consists of translational motions in three directions (surge, sway, and heave) and rotational motions about three axes (roll, pitch, and yaw), see Fig. 3(a). However, in this paper, only three motions (one translational motion and two rotational motions, that is, heave, roll, and pitch) are considered. This is due to that the loading/unloading operation requires the standing of both ships, and the mobile harbor is connected, by a special docking mechanism, to the mother ship that is stationary in the ocean due to its mega-size (Salvesen et al., 1970; Fossen, 1994; Xia et al., 1998; Neyes and Rodriguez, 2006; Selyam and Bhattacharyya, 2010). Therefore, the exciting force is only the Froude–Krilov force combined with the diffraction wave force. The drift force generated by wind and current is disregarded.

There are two approaches in obtaining the ship motions induced by random waves. First, the equations of motion derived by Newtonian or Lagrangian mechanics can be used (Fossen, 1994). The other approach is the response amplitude operators (RAOs) (Faltinsen, 1990). In this approach, RAOs are used to determine the likely behavior of a ship when operating at sea. In both cases, the ship hull shape is used and the developed model is tested in a model basin or by a specialized computer program.

In this paper, to simulate ship motions, the Marine Systems Simulator (MSS) toolbox (www.marinecontrol.org/) developed by Professor Thor I. Fossen's Team at Norwegian University of Science and Technology is used (Fossen and Smogeli, 2004; Perez and Fossen, 2007). This toolbox includes various models of ships, underwater vehicles, and floating structures. The library provides guidance, navigation, and control blocks for real-time simulation. Following the notation introduced by Fossen (1994),

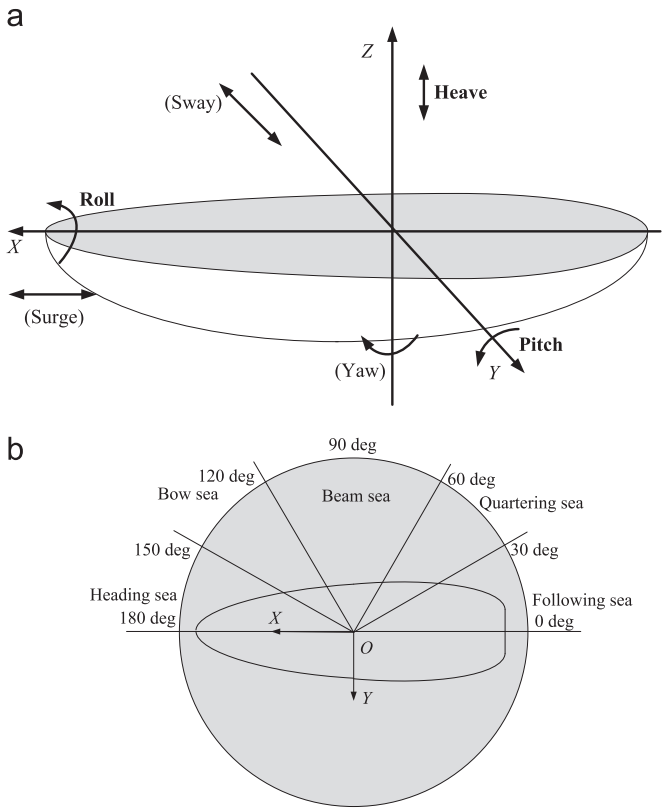

Fig. 3. The considered motions of the mobile harbor (heave, roll and pitch) and sea wave directions (Fossen, 1994). (a) Six DOF motions of the ship and (b) definition of sea wave directions.

the generalized coordinates of the ship is given by

$$\eta = [0,0,z,\phi,\psi,0]^T, \quad (4)$$

where z, ϕ, and ψ are the heave displacement, and the roll and pitch angles, respectively.

2.4. Equations of motion

Let m_t and m_p be the masses of the trolley and the payload (container), respectively. Let h be the crane height. Let x and y represent the position of the gantry and that of the trolley in the ship coordinate frame. Let l denote the rope length, and let θ and δ define the longitudinal and lateral sway angles of the load in the inertial coordinate frame. Finally, let f_y denote the control force applied at the trolley for trolley movement.

Given the ship motions (z, ϕ, ψ), the homogeneous transformation matrix from the ship coordinate frame to the inertial coordinate frame are obtained as follows:

$$T_n^s = \mathrm{Trans}(z_n,z)\mathrm{Rot}(y_n,\psi)Rot(x_n,\phi)$$

$$= \begin{bmatrix} \cos\psi & \sin\psi\sin\phi & \sin\psi\cos\phi & 0 \\ 0 & \cos\phi & -\sin\phi & 0 \\ -\sin\psi & \cos\psi\sin\phi & \cos\psi\cos\phi & z \\ 0 & 0 & 0 & 1 \end{bmatrix}, \quad (5)$$

where

$$\mathrm{Trans}(z_n) = \begin{bmatrix} 1 & 0 & 0 & 0 \\ 0 & 1 & 0 & 0 \\ 0 & 0 & 1 & z \\ 0 & 0 & 0 & 1 \end{bmatrix}, \quad \mathrm{Rot}(x_n,\phi) = \begin{bmatrix} 1 & 0 & 0 & 0 \\ 0 & \cos\phi & -\sin\phi & 0 \\ 0 & \sin\phi & \cos\phi & 0 \\ 0 & 0 & 0 & 1 \end{bmatrix},$$

$$\mathrm{Rot}(y_n,\psi)=\begin{bmatrix}\cos\psi & 0 & \sin\psi & 0\\ 0 & 1 & 0 & 0\\ -\sin\psi & 0 & \cos\psi & 0\\ 0 & 0 & 0 & 1\end{bmatrix}.$$

Then, the trolley position in the inertial coordinate frame is derived as follows:

$$p_T=\begin{bmatrix}\cos\psi & \sin\psi\sin\phi & \sin\psi\cos\phi & 0\\ 0 & \cos\phi & -\sin\phi & 0\\ -\sin\psi & \cos\psi\sin\phi & \cos\psi\cos\phi & z\\ 0 & 0 & 0 & 1\end{bmatrix}\begin{bmatrix}x\\ y\\ h\\ 1\end{bmatrix}$$
$$=\begin{bmatrix}x\cos\psi+y\sin\psi\sin\phi+h\sin\psi\cos\phi\\ y\cos\phi-h\sin\phi\\ z-x\sin\psi+y\cos\psi\sin\phi+h\cos\psi\cos\phi\\ 1\end{bmatrix}. \quad (6)$$

Using vector addition, the load position in the earth coordinate is also derived as follows:

$$p_L=p_T+\begin{bmatrix}-l\cos\theta\sin\delta\\ l\sin\theta\\ -l\cos\theta\cos\delta\\ 1\end{bmatrix}$$
$$=\begin{bmatrix}x\cos\psi+y\sin\psi\sin\phi+h\sin\psi\cos\phi-l\cos\theta\sin\delta\\ y\cos\phi-h\sin\phi+l\sin\theta\\ z-x\sin\psi+y\cos\psi\sin\phi+h\cos\psi\cos\phi-l\cos\theta\cos\delta\\ 1\end{bmatrix}. \quad (7)$$

By differentiating the positions of the trolley and the load in time, their velocities are derived as follows:

$$V_T=(V_{Tx},V_{Ty},V_{Tz})^T, \quad (8)$$

$$V_L=(V_{Lx},V_{Ly},V_{Lz})^T, \quad (9)$$

where

$$V_{Tx}=-x\dot\psi\sin\psi+\dot y\sin\psi\sin\phi+y\dot\psi\cos\psi\sin\phi+y\dot\phi\sin\psi\cos\phi+h\dot\psi\cos\psi\cos\phi-h\dot\phi\sin\psi\sin\phi,$$

$$V_{Ty}=\dot y\cos\phi-y\dot\phi\sin\phi-h\dot\phi\cos\phi,$$

$$V_{Tz}=\dot z-x\dot\psi\cos\psi+\dot y\cos\psi\sin\phi-y\dot\psi\sin\psi\sin\phi+y\dot\phi\cos\psi\cos\phi-h\dot\psi\sin\psi\cos\phi-h\dot\phi\cos\psi\sin\phi,$$

$$V_{Lx}=-x\dot\psi\sin\psi+\dot y\sin\psi\sin\phi+y\dot\psi\cos\psi\sin\phi+y\dot\phi\sin\psi\cos\phi+h\dot\psi\cos\psi\cos\phi-h\dot\phi\sin\psi\sin\phi-\dot l\cos\theta\sin\delta+l\dot\theta\sin\theta\sin\delta-l\dot\delta\cos\theta\cos\delta,$$

$$V_{Ly}=\dot y\cos\phi-y\dot\phi\sin\phi-h\dot\phi\cos\phi+\dot l\sin\theta+l\dot\theta\cos\theta,$$

$$V_{Lz}=\dot z-x\dot\psi\cos\psi+\dot y\cos\psi\sin\phi-y\dot\psi\sin\psi\sin\phi+y\dot\phi\cos\psi\cos\phi-h\dot\psi\sin\psi\cos\phi-h\dot\phi\cos\psi\sin\phi-\dot l\cos\theta\cos\delta+l\dot\theta\sin\theta\cos\delta+l\dot\delta\cos\theta\sin\delta.$$

Therefore, the kinetic and potential energies of the trolley and payload, respectively, are obtained as follows (Greenwood, 1987):

$$T=\tfrac{1}{2}m_t(V_{Tx}^2+V_{Ty}^2+V_{Tz}^2)+\tfrac{1}{2}m_p(V_{Lx}^2+V_{Ly}^2+V_{Lz}^2), \quad (10)$$

$$U=m_tg(z-x\sin\psi+y\cos\psi\sin\phi+h\cos\psi\cos\phi)+m_pg(z-x\sin\psi+y\cos\psi\sin\phi+h\cos\psi\cos\phi)-m_pgl\cos\theta\cos\delta. \quad (11)$$

Taking $q=(y,\theta,\delta)$ as the generalized coordinates corresponding to the generalized forces $f=(f_y,0,0)$ and using the Lagrange equation given by

$$\frac{d}{dt}\left(\frac{\partial T}{\partial\dot q_i}\right)-\frac{\partial T}{\partial q_i}+\frac{\partial U}{\partial q_i}=f_i,\quad i=1,2,3, \quad (12)$$

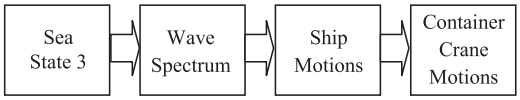

Fig. 4. Steps for simulating the crane dynamics upon Sea State 3.

Table 1
Simulation parameters.

Parameters	Values
Draught (m)	21
Breadth (m)	80
Length between perpendiculars (m)	115
Mass (kg)	5,197,800
Density of water (kg/m^3)	1025
Radius of gyration in roll (m)	33
Radius of gyration in pitch (m)	34
Radius of gyration in heave (m)	37.5
Acceleration of gravity (m/s^2)	9.81
Volume displacement (m^3)	50,712
Center of buoyancy w.r.t. baseline and Lpp/2 (m)	[0 0 7.2162]
Transverse metacentric height (m)	5.5284
Center of gravity w.r.t. baseline and Lpp/2 (m)	[0 0 20.5]
Crane height (m)	10
Rope length (m)	8
Trolley mass (kg)	6000
Payload (kg)	20,000
Gantry position (m)	5

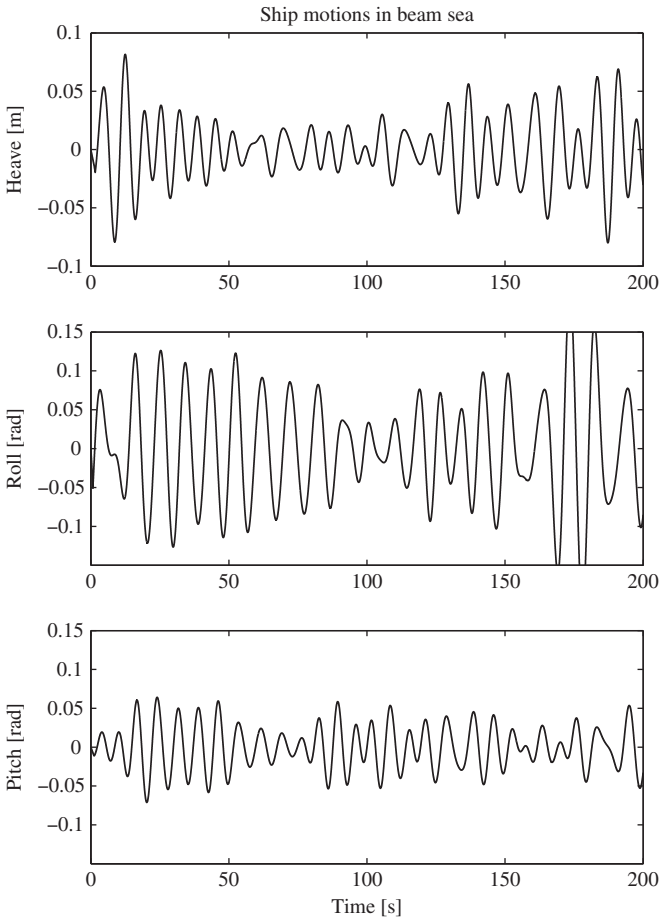

Fig. 5. Ship motions (heave, roll, and pitch) in the beam sea (simulation results).

the equations of motion of the trolley and the payload are obtained as follows:

$$(m_t+m_p)\ddot{y}+m_p l\ddot{\theta}(\sin\phi\sin\theta\cos(\delta-\psi)+\cos\phi\cos\theta)+m_p l\ddot{\delta}\sin\phi\cos\theta\sin(\delta-\psi)+c_1=f_y, \quad (13)$$

$$m_p(\sin\phi\sin\theta\cos(\delta-\psi)+\cos\phi\cos\theta)\ddot{y}+m_p l\ddot{\theta}+c_2=0, \quad (14)$$

$$m_p l\ddot{y}\sin\phi\cos\theta\sin(\delta-\psi)+m_p l^2\ddot{\delta}\cos^2\theta+c_3=0, \quad (15)$$

where

$$\begin{aligned}c_1 &= (m_t+m_p)(-x\ddot{\psi}\sin\phi-h\ddot{\phi}-h\dot{\psi}^2\sin\phi\cos\phi)\\ &+(m_t+m_p)(g+\ddot{z})\cos\psi\sin\phi-(m_t+m_p)(\dot{\psi}^2\sin^2\phi+\dot{\phi}^2)y\\ &+m_p\ddot{l}\cos\phi\sin\theta-m_p\ddot{l}\sin\phi\cos\theta\cos(\delta-\psi)\\ &+2m_p\dot{l}\dot{\delta}\sin\phi\cos\theta\sin(\delta-\psi)+2m_p\dot{l}\dot{\theta}\sin\phi\sin\theta\cos(\delta-\psi)\\ &+2m_p\dot{l}\dot{\theta}\cos\phi\cos\theta+m_p l(\dot{\theta}^2+\dot{\delta}^2)\sin\phi\cos\theta\cos(\delta-\psi)\\ &-m_p l\dot{\theta}^2\cos\phi\sin\theta-2m_p l\dot{\theta}\dot{\delta}\sin\phi\sin\theta\sin(\delta-\psi),\end{aligned}$$

$$\begin{aligned}c_2 &= m_p(2\dot{l}\dot{\theta}+2\dot{y}\dot{\psi}\sin\phi\sin\theta\sin(\delta-\psi)+2\dot{y}\dot{\phi}\cos\phi\sin\theta\cos(\delta-\psi)\\ &-2\dot{y}\dot{\phi}\sin\phi\cos\theta+2y\dot{\psi}\dot{\phi}\cos\phi\sin\theta\sin(\delta-\psi)\\ &-2h\dot{\psi}\dot{\phi}\sin\phi\sin\theta\sin(\delta-\psi)-y\dot{\phi}^2\cos\phi\cos\theta\\ &-y\dot{\phi}^2\sin\phi\sin\theta\cos(\delta-\psi)+h\dot{\phi}^2\sin\phi\cos\theta\\ &-h\dot{\phi}^2\cos\phi\sin\theta\cos(\delta-\psi)-y\dot{\psi}^2\sin\phi\sin\theta\cos(\delta-\psi)\\ &-x\dot{\psi}^2\sin\theta\sin(\delta-\psi)-h\dot{\psi}^2\cos\phi\sin\theta\cos(\delta-\psi)\\ &-x\ddot{\psi}\sin\theta\cos(\delta-\psi)+y\ddot{\psi}\sin\phi\sin\theta\sin(\delta-\psi)\\ &+h\ddot{\psi}\cos\phi\sin\theta\sin(\delta-\psi)-h\ddot{\phi}\cos\phi\cos\theta\\ &-h\ddot{\phi}\sin\phi\sin\theta\cos(\delta-\psi)+y\ddot{\phi}\cos\phi\sin\theta\cos(\delta-\psi)\\ &-y\ddot{\phi}\sin\phi\cos\theta+l\dot{\delta}^2\sin\theta\cos\theta+(g+\ddot{z})\sin\theta\cos\delta),\end{aligned}$$

$$\begin{aligned}c_3 &= m_p l(-2l\dot{\delta}\dot{\theta}\sin\theta\cos\theta+2\dot{l}\dot{\delta}\cos^2\theta+2\dot{y}\dot{\phi}\cos\theta\cos\phi\sin(\delta-\psi)\\ &-2\dot{y}\dot{\psi}\sin\phi\cos\theta\cos(\delta-\psi)-y\ddot{\psi}\sin\phi\cos\theta\cos(\delta-\psi)\\ &+y\ddot{\phi}\cos\phi\cos\theta\sin(\delta-\psi)-y(\dot{\phi}^2+\dot{\psi}^2)\sin\phi\cos\theta\sin(\delta-\psi)\\ &-2y\dot{\psi}\dot{\phi}\cos\phi\cos\theta\cos(\delta-\psi)-h\ddot{\psi}\cos\phi\cos\theta\cos(\delta-\psi)\\ &-h\ddot{\phi}\sin\phi\cos\theta\sin(\delta-\psi)-h(\dot{\phi}^2+\dot{\psi}^2)\cos\phi\cos\theta\sin(\delta-\psi)\\ &+2h\dot{\phi}\dot{\psi}\sin\phi\cos\theta\cos(\delta-\psi)-x\ddot{\psi}\cos\theta\sin(\delta-\psi)\\ &+x\dot{\psi}^2\cos\theta\cos(\delta-\psi)+(g+\ddot{z})\cos\theta\sin\delta).\end{aligned}$$

3. Simulation results

The ship motions and the sway angles of the container are simulated using MATLAB, in which the ship motions (z, ϕ, ψ) in (12)–(14) are generated using the MSS toolbox (Fossen and Smogeli, 2004). Three sea waves are considered: the heading sea ($\chi=180^\circ$) (or the following sea, $\chi=0^\circ$), the quartering sea ($\chi=45^\circ$) and the beam sea ($\chi=90^\circ$), see Fig. 3(b). Since the mobile harbor is stationary in the x (and y) direction, the heading sea and the following sea provide the same effects. Fig. 4 depicts the steps to generate the sway motions of the load. Table 1 shows

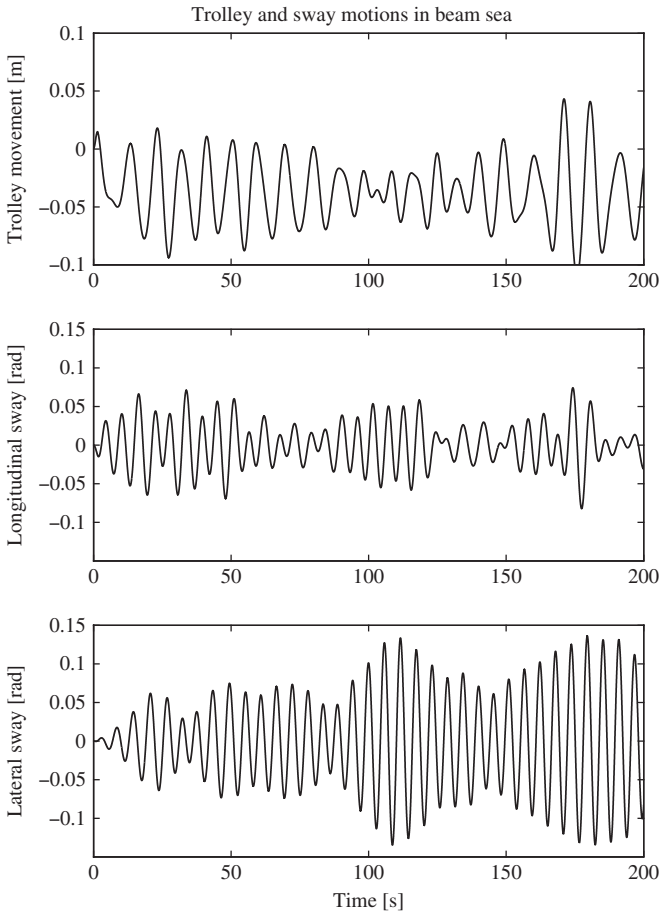

Fig. 6. Trolley movement and sway motions of the payload in the beam sea (simulation results).

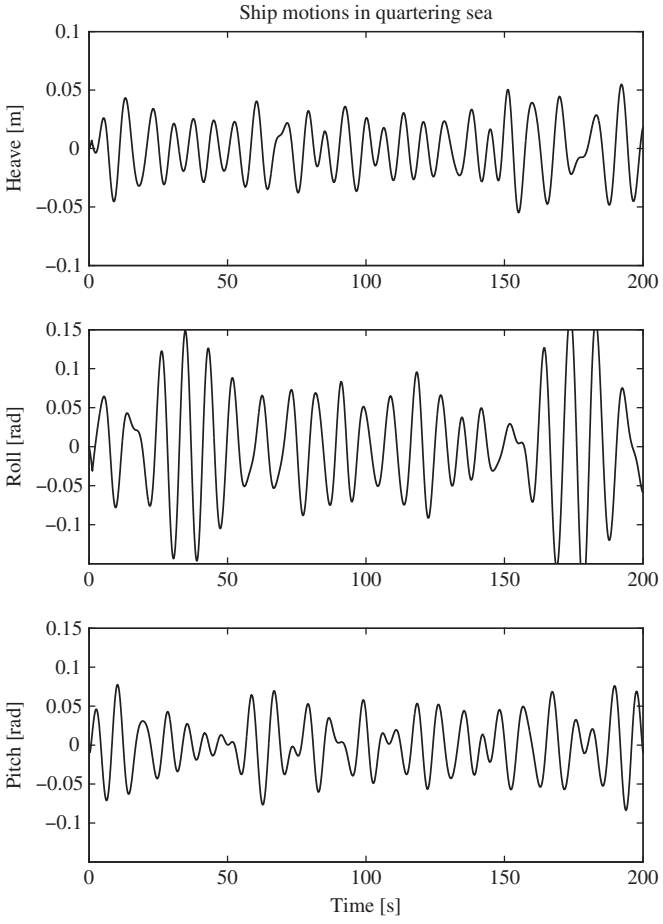

Fig. 7. Ship motions (heave, roll, and pitch) in the quartering sea (simulation results).

the parameters and their values used in simulation. Upon the ship motions (Figs. 5, 7, and 9) occurred in the Sea State 3 condition, the free motions of the trolley and the payload are simulated (Figs. 6, 8, and 10), which means that the brake system of the trolley is not used. This is to find out the coupling effect between the trolley and the payload dynamics. In real cases, however, an electrical or a mechanical brake system of the trolley will be active if it is not in motion, whereas the payload is in free motion.

From Figs. 5–10, the following observations are made. (i) In the beam sea, the rolling motion of the ship becomes the biggest and the pitching motion is the smallest, see Figs. 5, 7, and 9. The magnitude of the rolling motion is in the order of beam, quartering, and heading seas. (ii) However, the lateral sway angle of the load (which is normally caused by the pitching motion of the ship) becomes the biggest in the beam sea (see Fig. 6). The amplitude of the pitching motion of the ship in the heading sea is the biggest (see Fig. 9). This is due to, in the beam sea, that the lateral and the longitudinal sway motions of the load are coupled in the presence of large rolling motions of the ship. It is also noted that the lateral sway angle in the heading sea becomes the smallest. (iii) In the heading sea (see Fig. 9), the frequencies of the rolling and pitching motions of the ship become the smallest, which reflects the least excitation to the crane. (iv) In the mobile harbor operation, the lateral sway angle of the load caused by the sea waves may become a dominant one in comparison with the longitudinal sway angle occurred by the trolley movement.

From the above, the following important conclusions are made: (i) The suppression of the lateral sway angle of the load becomes a key issue (i.e., the conventional control methods will not work in suppressing the sways of the load on a mobile harbor) and the necessity for a new mechanism for the lateral sway control is needed. (ii) It is recommended that the mobile harbor operations for loading and unloading are made in the heading sea, suggesting a proper orientation of the mother ship in the ocean.

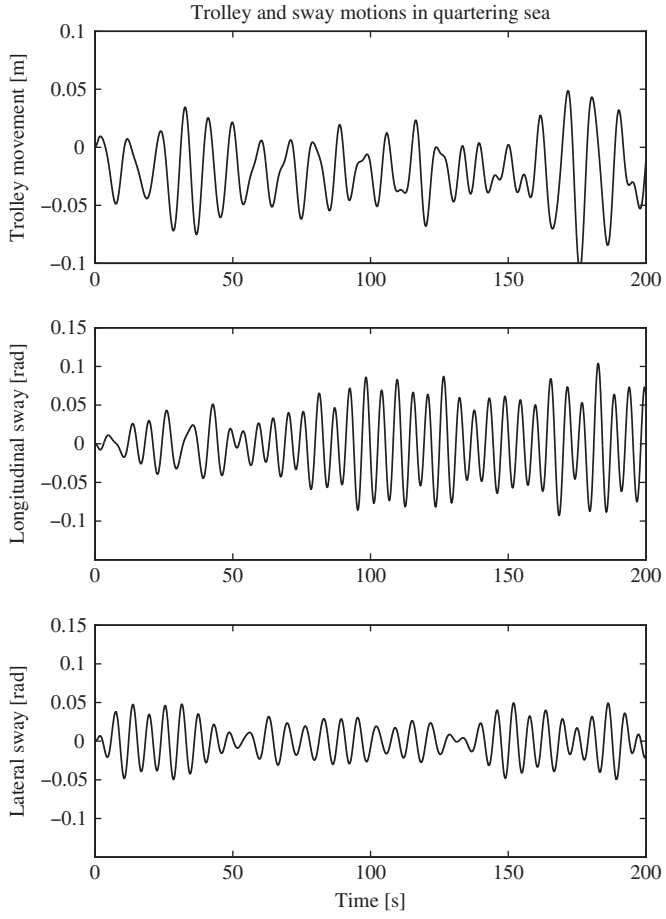

Fig. 8. Trolley movement and sway motions of the payload in the quartering sea (simulation results).

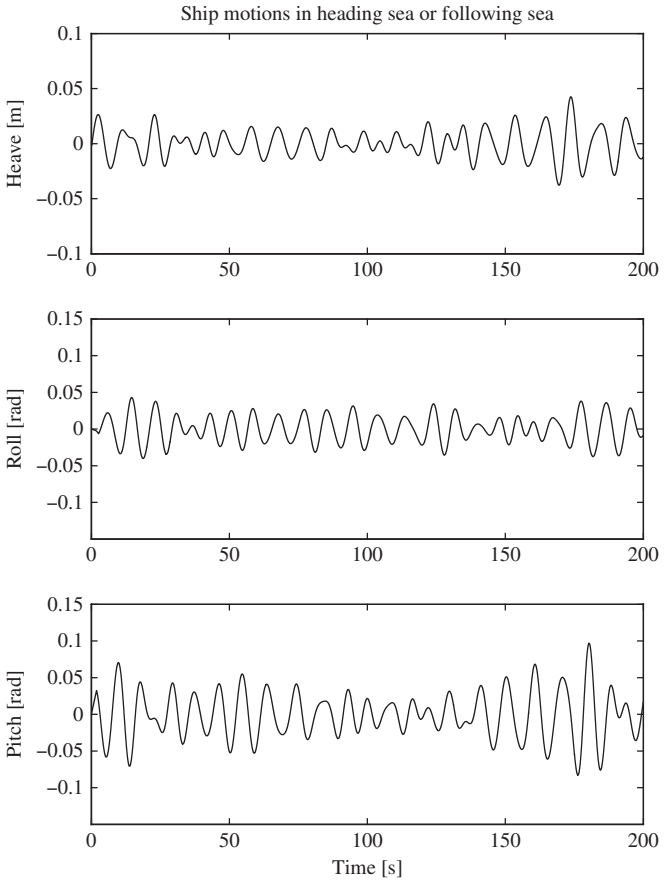

Fig. 9. Ship motions (heave, roll, and pitch) in the heading (or following) sea (simulation results).

4. Experimental results

The experimental setup consists of two subsystems: a six degree-of-freedom (DOF) Stewart platform to produce the ship motion induced by sea waves and a three-dimensional (3D) crane (INTECO, www.inteco.com.pl) to mimic the container crane on a mobile harbor. As seen in Fig. 11, the 3D crane is placed on top of the 6-DOF motion platform (Hong and Kim, 2000). To measure the motion of the platform, an IMU (inertial measurement unit) sensor (MTi sensor, XSENS) is used. The verification steps of the derived equations of motion of the crane are described as follows:

(I) First, see Fig. 12, the MSS is used to generate the ship motions induced by random waves (under Sea State 3 condition). Once the data of the ship motions (in this paper, only $[0,0,z,\phi,\psi,0]^T$ are used) are given, the lengths of the six legs of the platform are computed by solving the inverse kinematics problem of the motion platform.

(II) Then, the platform controller controls the leg lengths of the platform to replicate the ship motions given by the MSS. Also, the rotational angles of the platform are measured using the IMU sensor to use them for an independent verification of the crane dynamics. Fig. 13 compares the roll

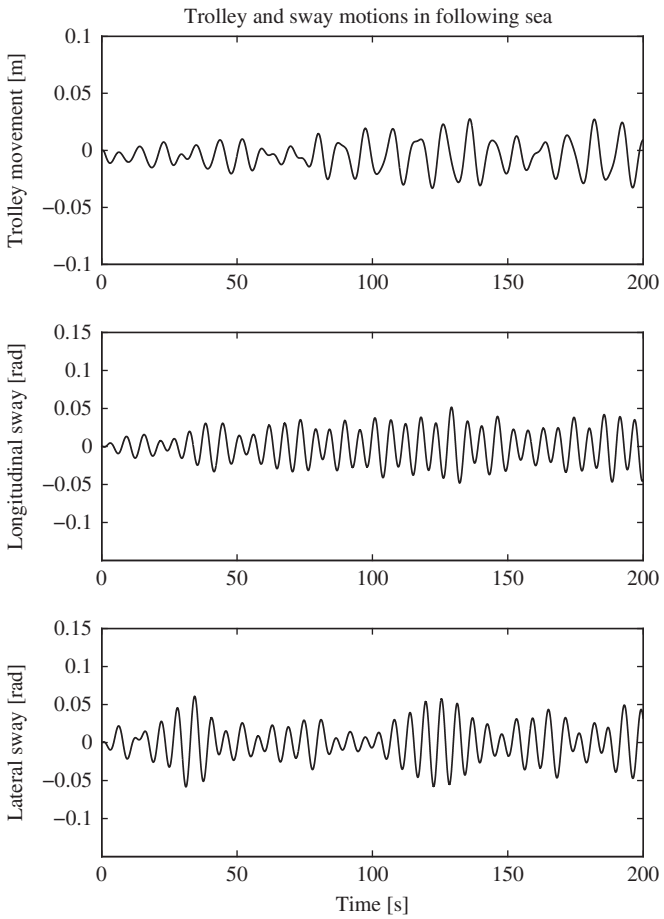

Fig. 10. Trolley movement and sway angles of the payload in the heading (or following) sea (simulation results).

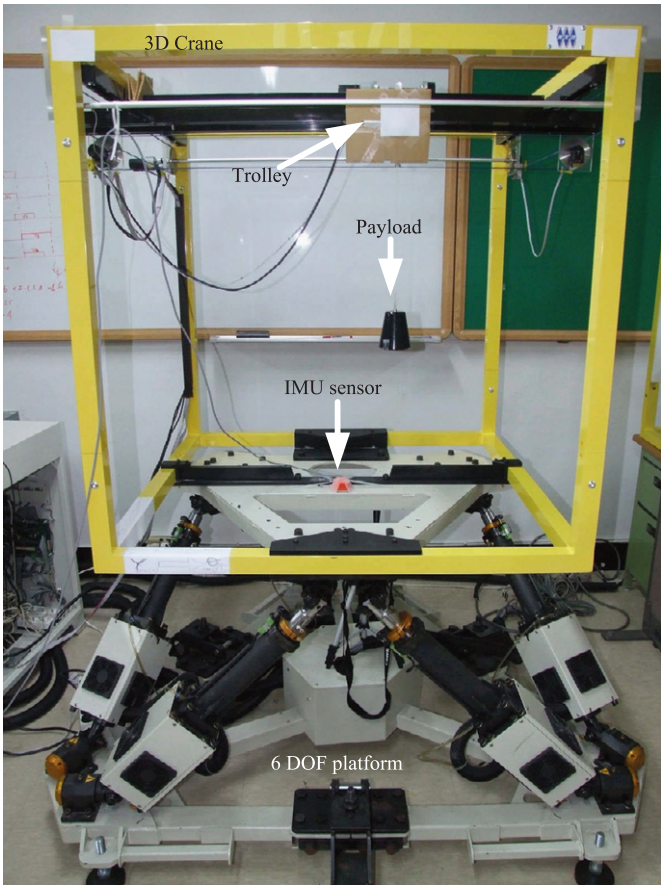

Fig. 11. Experimental setup: 6 DOF platform and 3D crane.

(ϕ) and pitch (ψ) motions of the ship between the simulation data from the MSS (reference) and the measured data from the IMU sensor. The obtained results reveal that the motion platform can reproduce the ship motions in Sea State 3 quite well.

(III) Now, to verify the correctness of the derived equations of motion of the crane, the subsequent procedure is split into two processes (see the lower part in Fig. 12): experiment using the 3D crane on the motion platform vs. simulation using the derived equations of motion in Section 2.4.

(IV) It is noted that even a sufficient closeness of the ship dynamics between simulation and motion platform has been revealed in Fig. 13(a) and (b), there is still a small discrepancy between these two, see Fig. 13(c). Therefore, for an independent verification of the crane dynamics from the ship dynamics, the provision of almost the same input conditions to the crane (between simulation and experiment) is pursued. For this, the measured platform motions are used to obtain the first and second derivative of the platform motions using the Kalman filter, which are again inputted to Eqs. (14) and (15) for simulation.

(V) Also, to separate the trolley dynamics from the sway dynamics of the load, the trolley position is assumed fixed in simulation and is actually fixed in experiment.

Finally, in Fig. 14, the sway motions of the payload measured using encoders and those simulated using (14) and (15) are compared. The simulation and experiment results of the

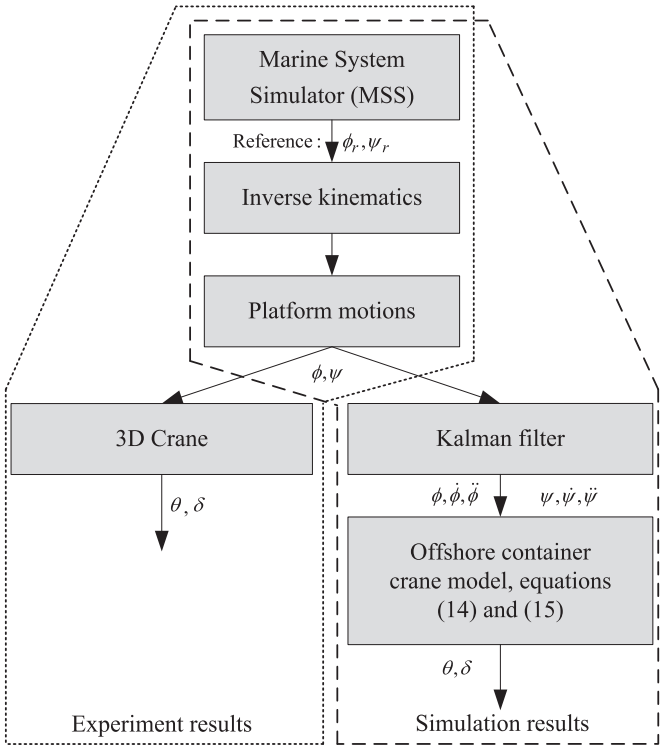

Fig. 12. Verification procedure.

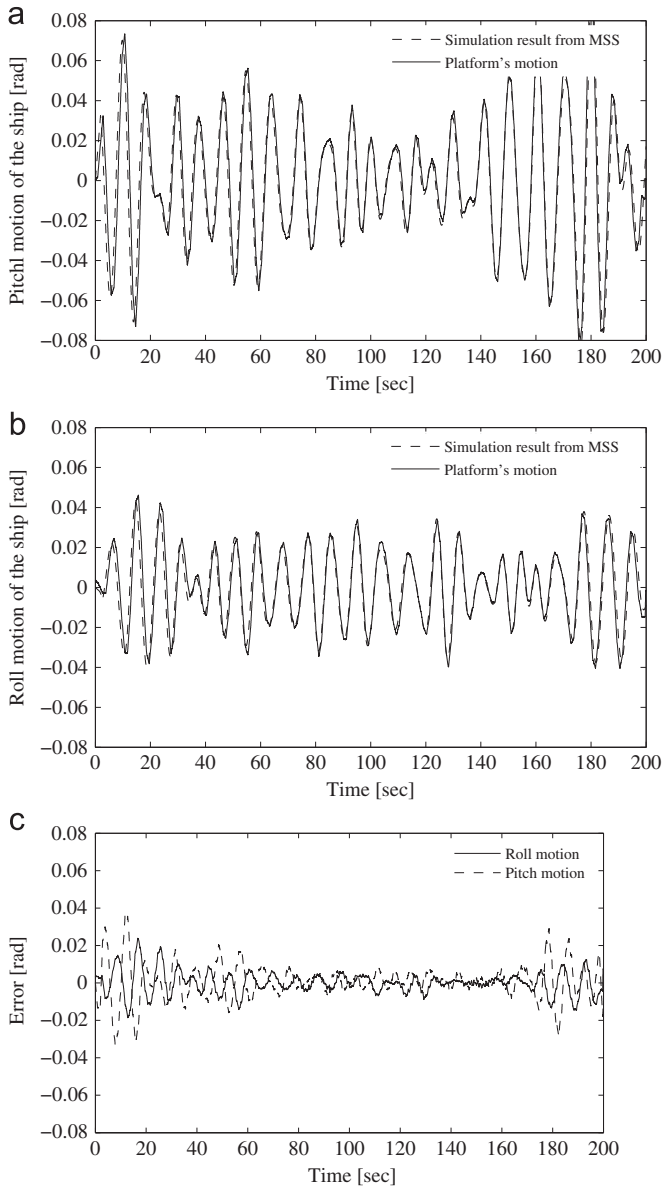

Fig. 13. Comparison of the ship motions in Sea State 3 (simulation vs. replicated motion in the platform). (a) Pitch motion of the ship, (b) roll motion of the ship and (c) error between simulation and replicated motion in the platform.

sway angles (longitudinal and lateral) are remarkably close. This reveals that the derived equations of motion of the crane are valid.

5. Conclusions

A dynamic model of a container crane mounted on a ship (called a "mobile harbor") was developed. The model included both sea-wave-induced ship motion and ship-motion-induced container sway. The Lagrange equation was applied to obtain the equations of motion of the trolley and the load. Heading sea (following sea), quartering sea and beam sea conditions were considered in simulation, the results of which show that when the ship is impacted by waves under those sea conditions, the container crane mounted on the ship will generate the sway angle of the payload. The waves coming from 90° will make more effects on the sway angles and it should be avoided in operating mobile harbors. The validation of the dynamics equation has been

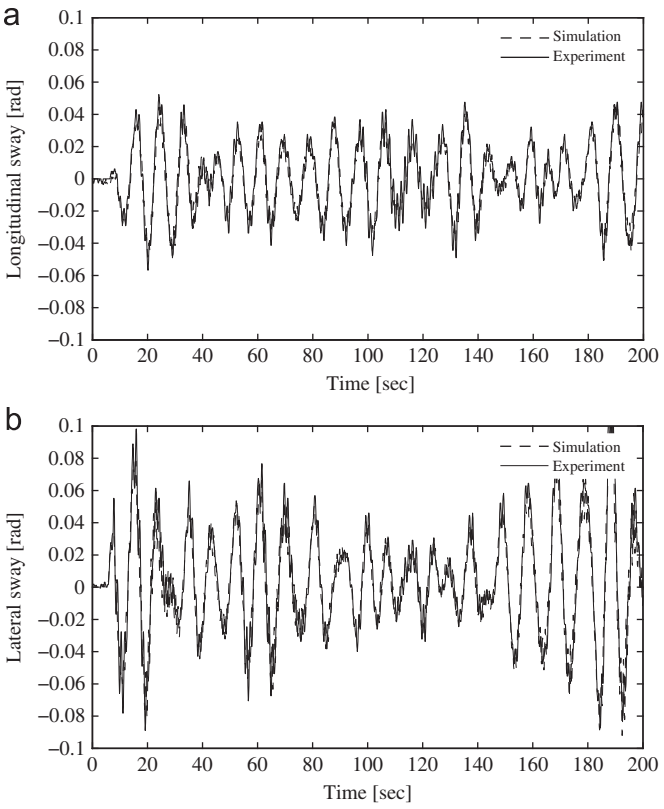

Fig. 14. Comparision of the sway motions of the payload (simulation vs. experimental result on the motion platform). (a) Longitudinal sway (θ) and (b) lateral sway (δ).

guaranteed through the comparison of the experiment and simulation results.

Acknowledgments

This work was supported by the Industrial Strategic Technology Development Program (Grant no. 10036235) named the Core Technology of a Light Crane (Mobile Harbor) funded by the Ministry of Knowledge Economy, Korea, and by the World Class University program funded by the Ministry of Education, Science and Technology through the National Research Foundation of Korea (Grant no. R31-20004).

References

Cha, J.H., Roh, M.I., Lee, K.Y., 2010. Dynamic response simulation of a heavy cargo suspended by a floating crane based on multibody system dynamics. Ocean Eng. 37 (14–15), 1273–1291.

Choi, J.Y., Hong, K.-S., Yang, K.-J., 2004. Exponential stabilization of an axially moving tensioned strip by passive damping and boundary control. J. Vib. Control 10 (5), 661–682.

Clauss, G., Stempinski, F., Dudek, M., Klein, M., 2009. Water depth influence on wave–structure-interaction. Ocean Eng. 36 (17–18), 1396–1403.

d'Andrea-Novel, B., Coron, J.M., 2000. Exponential stabilization of an overhead crane with flexible cable via a back-stepping approach. Automatica 36 (4), 587–593.

Do, K.D., Pan, J., 2008. Nonlinear control of an active heave compensation system. Ocean Eng. 35 (5–6), 558–571.

Ellermann, K., Kreuzer, E., 2003. Nonlinear dynamics in the motion of floating cranes. Multibody Syst. Dyn. 9 (4), 377–387.

Faltinsen, O.M., 1990. Sea Loads on Ships and Offshore Structures. Cambridge University Press, London.

Fang, Y., Dixon, W.E., Dawson, D.M., Zergeroglu, E., 2003. Nonlinear coupling control laws for an underactuated overhead crane system. IEEE/ASME Trans. Mechatronics 8 (3), 418–423.

Fossen, T.I., 1994. Guidance and Control of Ocean Vehicles. John Wiley & Sons, NewYork.

Fossen, T.I., Smogeli, Ø.N., 2004. Nonlinear time-domain strip theory formulation for low-speed manoeuvring and station-keeping. Modeling, Identification and Control 25 (4), 201–221.
Greenwood, D.T., 1987. Principles of Dynamics. Prentice Hall, Englewood Cliffs, NJ.
Hong, K.-S., Kim, J.G., 2000. Manipulability analysis of a parallel machine tool: application to optimal link length design. J. Robotic Syst. 17 (8), 403–415.
Hong, K.-S., Park, B.J., Lee, M.H., 2000. Two stage control for container. JSME Int. J. 43 (2), 273–282.
Kim, Y.-S., Hong, K.-S., Sul, S.-K., 2004. Anti-sway control of container cranes: inclinomer, observer, and state feedback. Int. J. Control Autom. Syst. 2 (4), 435–449.
Kim, C.-S., Hong, K.-S., 2009. Boundary control of container crane from the perspective of controlling an axially moving string system. Int. J. Control Autom. Syst. 7 (3), 437–445.
Kyoung, J.H., Hong, S.Y., Kim, J.W., Bai, K.J., 2005. Finite-element computation of wave impact load due to a violent sloshing. Ocean Eng. 32 (17–18), 2020–2039.
Lee, H.H., 2004. A new design approach for the anti-swing trajectory control of overhead cranes with the high-speed hoisting. Int. J. Control 77 (10), 931–940.
Lee, B.H., Park, J.C., Kim, M.H., Jung, S.J., Ryu, M.C., Kim, Y.S., 2010. Numerical simulation of impact loads using a particle method. Ocean Eng. 37 (2–3), 164–173.
Liu, D.T., Yi, J.Q., Zhao, D.B., Wang, W., 2005. Adaptive sliding mode fuzzy control for a two-dimensional overhead crane. Mechatronics 15 (5), 505–522.
Love, L.J., Jansen, J.F., Pin, F.G., 2003. Compensation of Wave-induced Motion and Force Phenomena for Ship-based High Performance Robotic and Human Amplifying System. Technical Report. US Department of Energy.
Neyes, M.A.S., Rodriguez, C.A., 2006. On unstable ship motions resulting from strong non-linear coupling. Ocean Eng. 33 (14–15), 1853–1883.
Ngo, Q.H., Hong, K.-S., 2009. Skew control of a quay container crane. J. Mech. Sci. Technol. 23 (12), 3332–3339.
Ngo, Q.H., Hong, K.-S., Jung, I.H., 2009. Adaptive control of an axially moving system. J. Mech. Sci. Technol. 23 (11), 3071–3078.
Ngo, Q.H., Hong, K.-S., 2012a. Adaptive sliding mode control of container cranes. IET Control Theory Appl. 6 (5), 662–668.
Ngo, Q.H., Hong, K.-S., 2012b. Sliding mode anti-sway control of an offshore container crane. IEEE/ASME Trans. Mechatronics 17 (2), 201–209.
Park, K.Y., Borthwick, A.G.L., Cho, Y.S., 2006. Two-dimensional wave–current interaction with a locally enriched quadtree grid system. Ocean Eng. 33 (2), 247–267.
Park, H., Chwa, D., Hong, K.-S., 2007. A feedback linearization control of container cranes: varying rope length. Int. J. Control Autom. Syst. 5 (4), 379–387.
Perez, T., 2005. Ship Motion Control: Course Keeping and Roll Stabilization Using Rudder and Fins. Springer, London.
Perez, T., Fossen, T.I., 2007. Kinematic models for manoeuvring and seakeeping of marine vessels. Model. Ident. Control 28 (1), 19–30.
Rahn, C.D., Zhang, F., Joshi, S., Dawon, D.M., 2000. Asymptotically stabilizing angle feedback for a flexible cable gantry crane. J. Dyn. Syst. Meas. Control 121 (3), 563–566.
Salvesen, N., Tuck, E.O., Faltinse, O., 1970. Ship motions and sea loads. Trans. Soc. Archit. Mar. Eng. 78 (6), 250–287.
Singhose, W., Porter, L., Kenison, M., Kriikku, E., 2000. Effects of hoisting on the input shaping control of gantry cranes. Control Eng. Pract. 8 (10), 1159–1165.
Singhose, W., Kim, D.R., 2008. Input shaping control of double-pendulum bridge crane oscillations. J. Dyn. Syst. Meas. Control 130 (2), 41–47.
Selyam, R.P., Bhattacharyya, S.K., 2010. System identification of coupled heave-pitch motion of ships with forward speed in random ocean waves. Ships Offshore Struct. 5 (1), 33–49.
VanZwieten, J.H., Driscoll, F.R., VanZwieten, T.S., Marikle, S.P., 2010a. Development of an adaptive disturbance rejection system for the rapidly deployable stable platform. Part 1: mathematical modeling and open loop response. Ocean Eng. 37 (8–9), 833–846.
VanZwieten, T.S., VanZwieten, J.H., Balas, M.J., Driscoll, F.R., 2010b. Development of an adaptive disturbance rejection system for the rapidly deployable stable platform. Part 2: controller design and closed loop response. Ocean Eng. 37 (14–15), 1367–1379.
Xia, J.Z., Wang, Z.H., Jensen, J.J., 1998. Nonlinear wave loads and ship responses by a time-domain strip theory. Mar. Struct. 11 (3), 101–123.
Zhu, G., Borthwick, A.G.L., Taylor, R.E., 2001. A finite element model of interaction between viscous free surface waves and submerged cylinders. Ocean Eng. 28 (8), 989–1008.